Marine Technology, Vol. 30, No. 4, Oct. 1993, pp. 286–296

A Resistance Study on a Systematic Series of Low *L/B* Vessels

Sander M. Calisal[1] and **Dan McGreer**[1]

Model resistance test results for a systematic series of low *L/B*, displacement-type vessels are presented. The UBC Series is based on West Coast seiners and trawlers. These vessels have low *L/B* and $L/V^{1/3}$ values that are outside the range of existing model series data. A parent hull form was developed that has 14 percent less resistance and yet has the same displacement and deck area of a typical fishing vessel. A series of 13 models was generated by systematically varying *L/B*, *B/T* and C_b. Algorithms are presented for calculation of the resistance of similar small vessels for two loading drafts. Results of side bulb applications reduced the resistance of the parent hull at design speed by an additional 16.6 percent. The parent hull form is designed as a developable hull form.

Introduction

Model series have proven to be very useful tools for predicting the resistance of ships. As part of a research program to reduce fuel consumption of fishing vessels a systematic model series has been developed at the University of British Columbia (UBC) based on a typical British Columbia purse seiner.

During the development of the UBC FISH [1][2] fuel consumption prediction program it was found that the resistance of many West Coast fishing vessels cannot be predicted by existing model series data (see Table 1). West Coast vessels typically have lower length-to-beam ratios and lower length-to-volume ratios than previously reported model series: British Ship Research Association (BSRA) Trawler Series [2,3], Webb Trawler Series [4,5,6], and the Technical University of Istanbul (ITU) Series [7]. Table 1 shows the comparison of vessel series parameters of these series.

The trend for new fishing vessels in British Columbia, Canada is to increasing beam for their length. The advantages of larger beam are increased fish hold volume, increased stability for hauling the net, larger deck area and the ability to carry a longer net drum. The disadvantage of larger beam is increased resistance. The series data could be used to calculate the tradeoffs of increasing beam with increasing resistance. Also, the series data will be useful in calculating the resistance of many existing small vessels.

A systematic series of models was generated from a parent hull form. The series parent was developed by testing different chine, stern and bow configurations to find a hull with the lowest resistance. This hull was selected as the series parent and was scaled to generate a systematic series of 13 models. The series was created by varying the length-to-beam ratio, beam-to-draft ratio, and the block coefficient.

Resistance prediction algorithms have been developed by a regression analysis of the model test results. The algorithms are suitable for implementation on computer and are presently used in the UBC FISH program.

Table 1 Comparison of fishing vessel series parameter ranges

Series	C_b	L/B	B/T	$L/V^{1/3}$
UBC	.53 - .61	2.6 - 4.0	2 - 3	3 - 4.47
BSRA	.53 - .63	4.3 - 5.8	2 - 3	4.35 - 5.1
ITU	.35 - .56	3.3 - 5	2 - 3.2	3.4 - 6.1
Webb	.42 - .53	3.2 - 5.75	2.3	3.85 - 5.22

Model test procedure

The resistance experiments were conducted at the BC Research Ocean Engineering Centre located adjacent to the UBC campus. The towing tank is 67.06 m (220 ft) long, 3.66 m (12 ft) wide, and 2.44 m (8 ft) deep. The models were constructed of wood and were between 1.52 m (5 ft) and 2.13 m (7 ft) long. They were built at a scale of 13.75:1.

The models were tested at about ten speeds in the Froude number range of 0.2 to 0.45, which corresponds to full-scale speeds of between 6 and 12 knots. Two drafts were tested: light ship and loaded. The light ship draft is defined as the draft the vessel would have when departing for the fishing grounds. The fishholds are assumed to be empty and a full supply of fuel and stores is assumed. At the loaded draft, it is assumed that the fishholds would be full and a half supply of fuel and stores would be onboard.

The models were towed from a bracket located at midships (station 5). The bracket was fastened as low as possible so that trim moments caused by towing would be minimized. The models were free to squat and trim. Resistance was measured by a strain gage force dynamometer and the sinkage and trim were measured by high-resolution potentiometers.

To induce a turbulent boundary layer on the models, brass studs were inserted at 25.4 mm (1 in.) centers 10% of *LBP* aft of the forward perpendicular. The pins were 3.18 mm (0.125 in.) in diameter and extended 2.54 mm (0.1 in.) from the hull surface. The ITTC-57 (International Towing Tank Conference) correlation line was used to estimate the friction drag. The resistance equations are:

$$C_f = \frac{0.075}{(\log_{10}\mathrm{Rn} - 2)^2}$$

[1] Professor and research engineer, respectively, Mechanical Engineering Department, University of British Columbia, Vancouver, BC, Canada.

[2] Numbers in brackets designate References at end of paper.

Presented to the May 11/12, 1990 Spring Meeting of the Pacific Northwest Section of The Society of Naval Architects and Marine Engineers.

0025-3316/93/0030-0286$00.47/0

$$C_r = C_t - C_f(1 + k)$$

$$R_n = \frac{VL}{\nu}$$

A form factor was used in the scaling of the light ship draft results but was not used in the scaling of the loaded-draft results. The form factor was found by making a Prohaska plot based on four low-speed resistance tests. The calculated form factors are listed in Table 2 and are presented in the form $(k+1)$. The form factors measured are found to be smaller than those predicted by the algorithm given in the *Principles of Naval Architecture* on page 91, Vol. II [10]. The values predicted for $k+1$ by this algorithm were higher than the measured values by about 8 percent. The authors suggest that the users should calculate the model resistance based on the information available in this paper and follow a model to ship scaling procedure with a form factor of their own choice. In the loaded-draft case, the form factor was assumed to be zero for the algorithmic calculations. The towing tank procedure was calibrated by testing a Wigley hull and a Series 60 block 60 model; satisfactory results were obtained.

Parent hull development

The first step in the generation of the UBC Series was to develop the parent hull form. The starting point for the development of a parent for the series was a fishing vessel hull that had been designed by Gerry Stensgaard at BC Research. It was a 21.34 m (80 ft) purse seiner typical of steel and aluminum vessels currently being constructed on the West Coast of North America for purse seining of salmon and herring (Fig. 1). The principal particulars of the vessel are given in Table 3.

Purse seining is a stationary fishing method in which a large net is deployed in a circle surrounding a school of fish. The net is then drawn closed on the bottom and the net reeled in over the stern. These vessels typically have low L/B ratios for large hold capacity, maneuverability and stability.

A number of model tests were conducted to ensure that the parent hull would have good resistance characteristics. The first experiment was to determine if modifying the hull to have a double chine or round bilge would reduce the resistance. Two models were designed so that the area of each station and waterline breadth at each station remained constant. This ensured that all the sectional area curve, displacement, form coefficients, and center of buoyancy remained unchanged. The wetted surface also did not change significantly. The wetted surface of the double chine hull was 1.2% greater than the single chine hull and the round bilge hull was 0.2% greater than the single chine hull. The body plans of the three hulls are shown in Fig. 2. A significant reduction in resistance was achieved with the double chine and round bilge designs (Fig. 3). At a typical cruising speed of 10.5 knots the resistance was reduced 8% for the double chine hull and 10% for the round bilge hull. Because it had performance that nearly matched the round bilge design, and probably would cost less to construct, the double chine hull was selected for further refinement.

Additional experiments were then conducted to improve the double chine hull. Gireesh Sadasivan, a graduate student, designed a developable new bow shape that reduced the half entrance angle from 42 to 30 deg (Fig. 4). The sectional areas of each station were again held constant but the design waterline half-breadths were reduced in the bow region to reduce the entrance angle. To maintain the same sectional area curve, the profile of the bow was made deeper and the stem was made vertical below the design waterline. The stern profile was also modified. The run angle was decreased by making the buttocks slightly concave (hooked buttocks).

The resistance decreased slightly when compared with the previously tested double chine hull (see Fig. 5). Measurements of the wave profiles by longitudinal cut procedures indicated that the bow wave had been significantly reduced by the new bow shape but, since the reduction in resistance was less than expected, it was concluded that the new bow may have had favorable resistance characteristics but the new stern did not. A new model was constructed that had the new bow and the original double chine model stern. This configuration achieved a reduction of 7% at 10.5 knots over the double chine hull or 14% when compared with the single chine hull (Fig. 5). This hull was then selected to be the parent hull form for the UBC fishing vessel series (Fig. 6). Offsets for the UBC Series parent hull are given in Appendix 1. The geometric properties of the parent hull are given in Table 2.

Table 2 Geometric properties of UBC Series models

Geometric Properties of UBC Series at Loaded Draft										
Model	L (m.)	W_s (m^2)	L/B	B/T	C_b	C_p	C_m	L/V	LCB/L	LCF/L
1	1.552	1.125	3.06	2.49	0.615	0.700	0.878	3.36	3.74%	7.10%
2	1.319	0.956	2.60	2.49	0.615	0.700	0.878	3.01	3.74%	7.10%
3	2.017	1.462	3.98	2.49	0.615	0.700	0.878	4.00	3.74%	7.10%
4	1.552	0.948	3.06	2.99	0.615	0.700	0.878	3.57	3.74%	7.10%
5	1.552	1.124	3.06	1.99	0.615	0.700	0.878	3.12	3.74%	7.10%
6	2.017	1.232	3.98	2.99	0.615	0.700	0.878	4.25	3.74%	7.10%
7	1.552	1.016	3.06	2.49	0.531	0.653	0.813	3.53	3.47%	6.16%
8	2.017	1.321	3.98	2.49	0.531	0.653	0.813	4.20	3.47%	6.16%
9	1.552	0.929	3.06	2.99	0.531	0.653	0.813	3.75	3.47%	6.16%
10	1.552	1.150	3.06	1.99	0.531	0.653	0.813	3.27	3.47%	6.16%
11	2.017	1.461	3.98	1.99	0.615	0.700	0.878	3.71	3.74%	7.10%
12	2.017	1.208	3.98	2.99	0.531	0.653	0.813	4.46	3.47%	6.16%
13	2.017	1.496	3.98	1.99	0.531	0.653	0.813	3.90	3.47%	6.16%

Geometric Properties of UBC Series at Lightship Draft											
Model	L (m.)	W_s (m^2)	L/B	B/T	C_b	C_p	C_m	L/V	LCB/L	LCF/L	1+k
1	1.552	0.914	3.06	3.52	0.531	0.631	0.842	3.96	1.58%	6.54%	1.08
2	1.319	0.777	2.60	3.52	0.531	0.631	0.842	3.55	1.58%	6.54%	1.28
3	2.017	1.188	3.98	3.52	0.531	0.631	0.842	4.72	1.58%	6.54%	0.98
4	1.552	0.855	3.06	4.23	0.531	0.631	0.842	4.21	1.58%	6.54%	1.08
5	1.552	1.004	3.06	2.81	0.531	0.631	0.842	3.67	1.58%	6.54%	1.11
6	2.017	1.112	3.98	4.23	0.531	0.631	0.842	5.02	1.58%	6.54%	1.17
7	1.552	0.822	3.06	3.52	0.447	0.598	0.747	4.19	1.61%	5.77%	1.08
8	2.017	1.068	3.98	3.52	0.447	0.598	0.747	5.00	1.61%	5.77%	1.10
9	1.552	0.763	3.06	4.23	0.447	0.598	0.747	4.46	1.61%	5.77%	1.32
10	1.552	0.913	3.06	2.81	0.447	0.598	0.747	3.89	1.61%	5.77%	1.27
11	2.017	1.305	3.98	2.81	0.531	0.631	0.842	4.38	1.58%	6.54%	1.13
12	2.017	0.992	3.98	4.23	0.447	0.598	0.747	5.31	1.61%	5.77%	1.13
13	2.017	1.187	3.98	2.81	0.447	0.598	0.747	4.64	1.61%	5.77%	1.06

Nomenclature

B = waterline beam at amidships
C_b = block coefficient
C = frictional resistance coefficient
C_m = midships area coefficient
C_p = prismatic coefficient
C_r = residual resistance coefficient
C = total resistance coefficient
F_n = Froude number
L = waterline length
LCB = longitudinal center of buoyancy
R_n = Reynolds number
R_r = residual resistance
R = total resistance in Newtons
T = draft at midships excluding keel
U = ship speed
V = displaced volume
W_s = wetted surface area in calm water
g = gravitational acceleration
k = form factor
ν = kinematic viscosity coefficient
Δ = displacement of hull

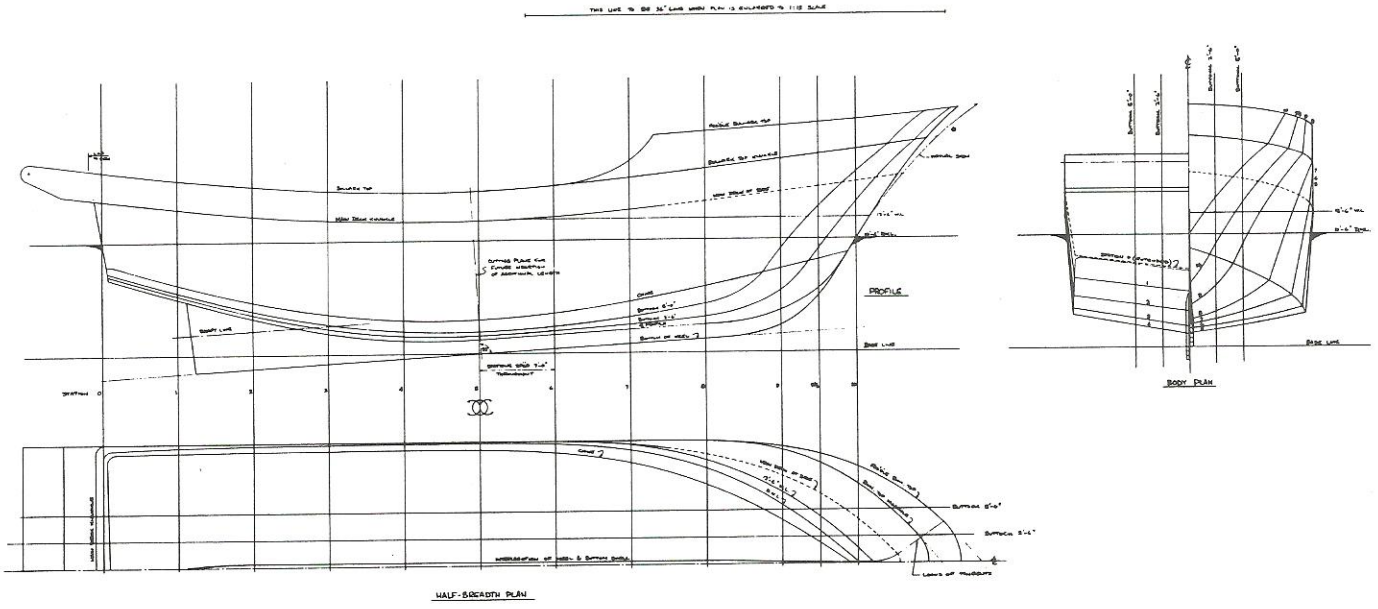

Fig. 1 Lines plan of single-chine seiner

Table 3 Principal particulars of a typical seiner

Length Between Perpendiculars	21.34 m.	(70 ft.)
Molded Beam	7.01 m.	(23 ft.)
Draft excluding keel	2.80 m.	(9.2 ft.)
Displacement	265 tonnes	(260 L.T.)
C_b	.615	
C_p	.700	
C_m	.878	

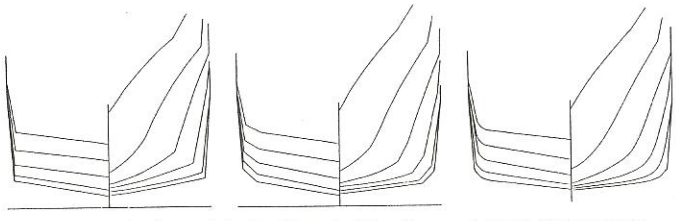

Fig. 2 Body plans of single-chine, double-chine, and round-bilge models

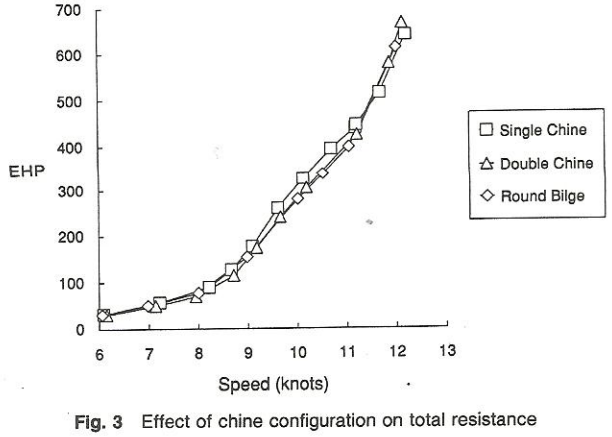

Fig. 3 Effect of chine configuration on total resistance

The parent hull is referred to in the table as model 1 and is intended to be a developable hull form.

Tests of series models

Once established, the parent hull design was scaled in length and depth to generate models in a systematic series of seven models (Fig. 7). The L/B ratio was increased by 30% and decreased by 15%. The B/T ratio was both increased and decreased by 20%. The models were generated by holding the beam constant and scaling the length to change the L/B ratio and scaling the depth to change the B/T ratio. This could be done easily by computer and model scale drawings were generated on a large Houston plotter for the model builder.

The geometric properties of the models for both light ship and loaded drafts are given in Table 2. Scaling the length and depth of the model did not alter C_b, C_m, C_p or LCB/L. In order to determine the effect of changing the block coefficient a scaling function was developed that when applied to the parent hull offsets decreased the block coefficient by 14% at the loaded draft and 16% at the light ship draft (Fig. 8). The equation used to scale half-breadths was:

$$y_{new} = y\left\{\left[0.2\frac{z}{T} + 0.8\right]\left[1 - 1.2\left(\frac{x}{L}\right)^2\right]\right\}$$

where

x = distance forward or aft of midships
y = half-breadth
z = height above baseline

Scaling the hull to reduce the block coefficient also reduced the midship section coefficient and the prismatic coefficient. The scaling did not change the LCB or LCF significantly. The new block coefficient hull was then scaled in the same way as the original block coefficient hull to generate six additional models with different L/B and B/T ratios.

The results from the resistance tests of both drafts are presented in tables and graphs in Appendix 2. The results are presented as graphs of residual resistance coefficient versus Froude number. The ITTC-57 correlation line is used to obtain

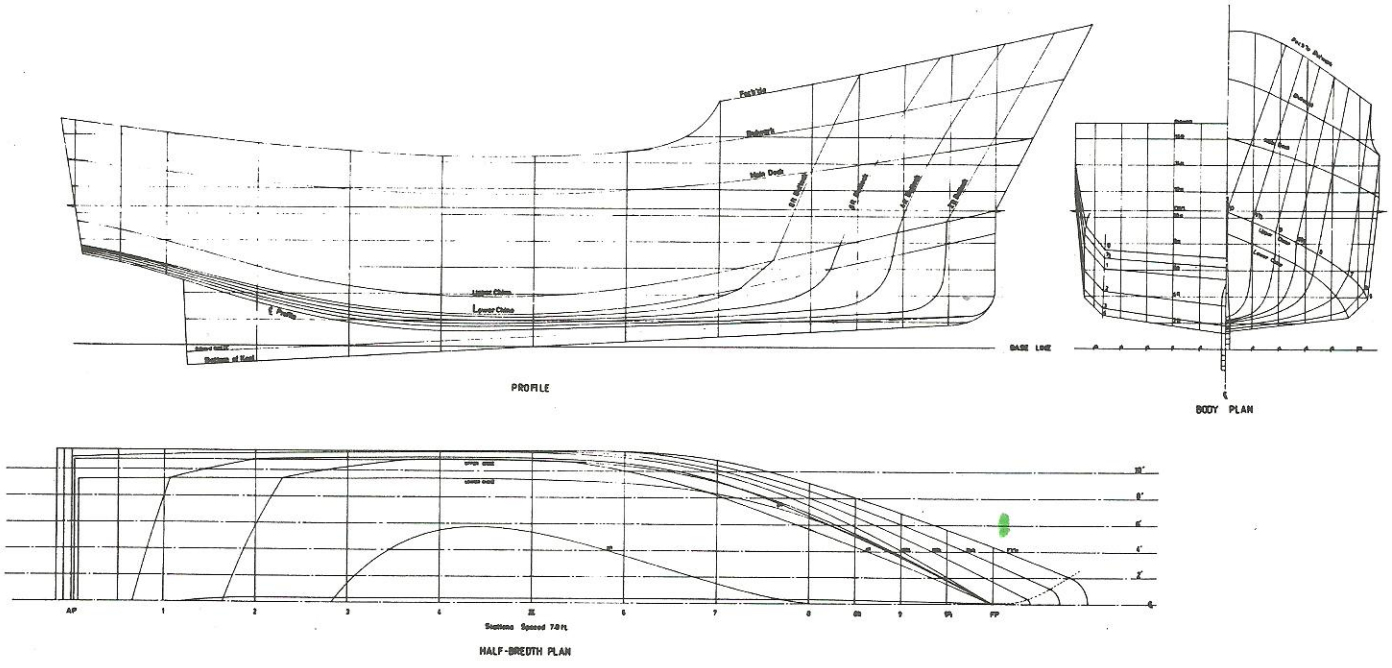

Fig. 4 Lines plan of second double-chine model with new bow and stern

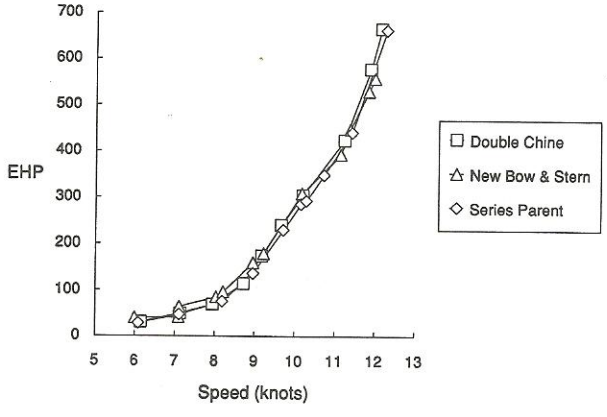

Fig. 5 Resistance optimization of parent hull

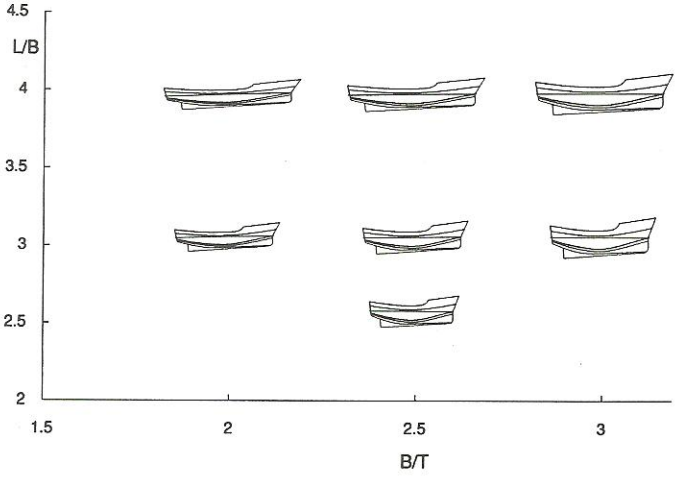

Fig. 7 UBC Series model parameter matrix

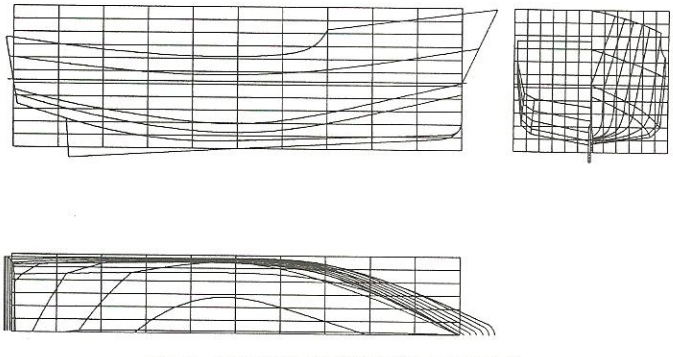

Fig. 6 Lines plan of UBC Series parent hull

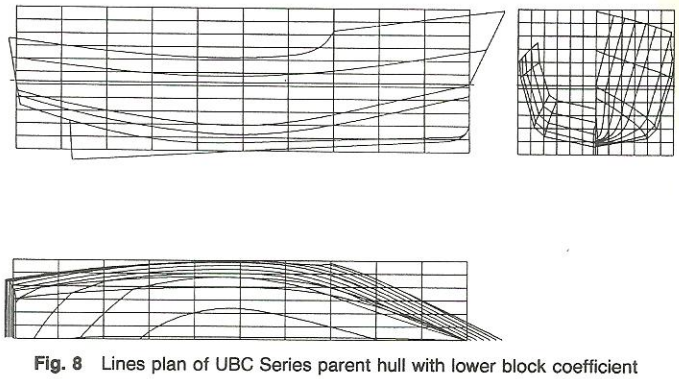

Fig. 8 Lines plan of UBC Series parent hull with lower block coefficient

the residual resistance values. Also shown in the graphs are estimates for the residual resistance calculated using the resistance algorithms presented in the following section.

Development of resistance algorithm

Two resistance algorithms have been developed based on regression analysis of the model test data. The first algorithm is based on the equation developed by Oortmerssen [8,10] for the analysis of small vessels and the second is an equation developed at the Institute of Marine Dynamics (IMD), St. Johns, Newfoundland [11] for semi-planing hulls. The Oortmerssen equation was found to have the best fit for the loaded-draft resistance data and the IMD equation was best for the light ship draft data.

The Oortmerssen equation is based on Havelock's equation for wave resistance of a two-dimensional pressure disturbance (the vessel is replaced by a pressure point at the bow and a negative pressure point at the stern):

$$C_r = C_1 e^{-m/9F_n^2} + C_2 e^{-m/9F_n^2} + C_3 e^{-m/F_n^2} \sin F_n^2 + C_4 e^{-m/F_n^2} \cos F_n^2$$

where

$$C_i = d_{i,0} + d_{i,1}\frac{L}{B} + d_{i,2} + d_{i,3}\frac{B}{T} + d_{i,4}$$

and

$$m = 0.14347\, C_p^{-2.1976}$$

The coefficients $d_{i,j}$ were determined from regression analysis of the model test data. Two sets of coefficients were computed, one for each block coefficient. This was found to give a much better fit to the model test data.

The coefficients for C_b=0.615 are given in Table 4 and those for C_b=0.531 in Table 5. Oortmerssen's coefficients for the equation for m were used in the analysis.

Table 4 Coefficients for resistance algorithm for C_b = 0.615

i=	1	2	3	4
$d_{i,0}$	.074654	.076958	-.000162	-.018642
$d_{i,1}$	.001879	$7.7\ 10^{-5}$	$7.42\ 10^{-5}$	$1.05\ 10^{-5}$
$d_{i,2}$	-.000701	$1.8\ 10^{-5}$	.000907	.000119
$d_{i,3}$	-.05158	-.005247	-.001137	-.001944
$d_{i,4}$	.009871	.000572	-.000661	.001169

Table 5 Coefficients for resistance algorithm for C_b = 0.531

i=	1	2	3	4
$d_{i,0}$	.006056	.166001	-.067109	-.047944
$d_{i,1}$	$1.42\ 10^{-6}$	-.000817	.000425	.000326
$d_{i,2}$	$9.99\ 10^{-6}$	-.005752	.00299	.002295
$d_{i,3}$	-.001758	-.00068	.000302	.000147
$d_{i,4}$	.000246	-.002688	.001521	.00118

The accuracy of the resistance algorithms is shown in Appendix 2. For each model, residual resistance coefficient C_r versus Froude number is plotted. The results from the Oortmerssen equation are labeled "eqn 1". The calculated resistance values are reasonably close to the model data for all of the models. For the C_b=0.615 equation, 86 regression data points were used, resulting in an average error in prediction of the total resistance of 4.6%; for the C_b=0.531 equation, 54 points were used, giving an average error of 6.4%. There are two limitations to this resistance algorithm. The algorithm smooths out the hump in the resistance curve at a Froude number around 0.35 and the algorithm is not accurate above Froude number 0.425.

The IMD algorithm uses the equation

$$\frac{R_r}{\Delta} = \frac{1}{C_b\frac{LL}{BT}}(a_1 + a_2 F_n + a_3 F_n\frac{B}{T} + a_4 S^2 + a_5 F_n\frac{B}{T}S^2 + a_6 F_n^5 + a_7 F_n^5 S + a_8 F_n^5 S^2 + a_9 F_n^8 S + a_{10} F_n^{10} + a_{11} F_n^{10} S^2)$$

where

$$S = L^2/BT.$$

A set of coefficients a_i was computed by regression analysis for each of the two draft conditions. The coefficients for the loaded draft are given in Table 6 and for the light ship draft in Table 7.

The plots in Appendix 2 labeled "eqn 2" refer to the prediction by the IMD method using the coefficients in Table 6. The curves labeled "eqn 3" are for light condition and they refer to the IMD equation with coefficients from Table 7.

An algorithm for the estimation the wetted surface areas is

$$S = L(2T + B)\sqrt{C_m}\left(c_1 + c_2 C_B + c_3 C_m + c_4\frac{B}{T}\right)$$

where the coefficients were derived as c_1 = 0.750, c_2 = −0.155, c_3=0.161, and c_4=−0.001 for the parent hull form (C_B=0.615, C_m=0.878) in the loaded condition. It was found that the maximum deviation from the measured wetted surface for the models is of the order 5 percent.

Table 6 Coefficients for IMD equation for loaded draft

a_1	.01350916	a_7	.9437698
a_2	.2399775	a_8	-1.076558×10^{-2}
a_3	-.1094626	a_9	.1599635
a_4	-7.249616×10^{-5}	a_{10}	2.006548×10^{-3}
a_5	1.413843×10^{-4}	a_{11}	.6638434
a_6	7.075775×10^{-2}		

Table 7 Coefficients for IMD equation for light ship draft

a_1	1.850581×10^{-2}	a_7	.811856
a_2	-2.308092×10^{-2}	a_8	-.0085882
a_3	-1.926078×10^{-2}	a_9	.1251543
a_4	-1.144379×10^{-5}	a_{10}	9.04941×10^{-4}
a_5	2.111938×10^{-5}	a_{11}	.7494847
a_6	4.297524×10^{-2}		

Effect of bulbous bows on the series parent hull

Further testing of the UBC Series parent hull has shown that it is responsive to the addition of a bulbous bow. Pioneering work on this type of bulb was done by Weinblum [12] and Hsuing [15] but never considered for hull forms like fishing vessels. The main idea was that they should work well with fine hull forms. Several experiments were conducted with side bulbs [9]. Side bulbs protrude to the side rather than forward as with a conventional bulbous bow (Fig. 9). Four bulb shapes were developed for the UBC Series parent using the OPTIHULL computer program developed at UBC by Goren [9]. This procedure permits the design of bulbs for operation at different drafts and speeds very suitable for fishing vessels.

The mathematical methods used to develop the side bulb designs are described in reference [9]. Briefly, the method optimizes an objective function which is the sum of the frictional resistance and the wave resistance. The frictional resistance is estimated by the ITTC-1957 formula and the wave resistance by Michell's integral. The hull surface is represented by tent functions, leading to a resistance equation that is a function of the hull offsets. The quadratic programming method is used to find the offsets that give the minimum resistance. Constraints are used in the optimization to limit the offsets to practical values. It is shown that the proper selection of constraints in the formulation is essential for a practical bulb form and nonseparating flow aft of the bulb. Some additional results are discussed in [14], and Susuki [13] developed a different procedure to design side bulbs and applied his procedure successfully on the UBC parent hull.

As an example, the results for Bulb 2 are given in Fig. 10, which shows that at speeds above 9 knots the resistance is substantially reduced. At a typical cruising speed of 10.5 knots the resistance was reduced 16.6%. At speeds below 9 knots the resistance increased somewhat. Experimentally observed wave-breaking aft of the side bulb seems to have caused the increase in resistance at low speeds.

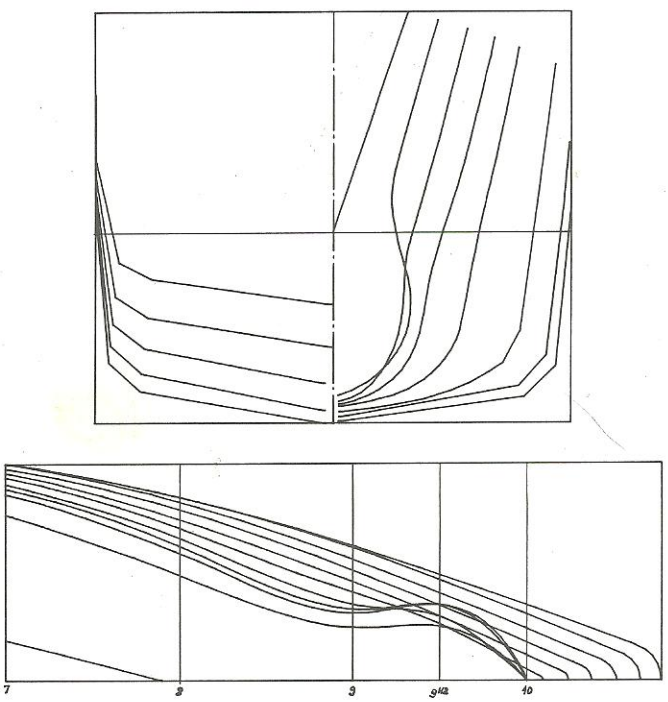

Fig. 9 Lines plan of side bulb 2

Conclusions

The resistance algorithm presented in this paper will be useful for estimating the resistance of low L/B displacement vessels, for which resistance data have not previously been available. The systematic series is based on a West Coast seiner; however, it is applicable to other types of small vessels.

Tests to optimize the hull form of the UBC series parent have indicated that significant reductions in resistance are possible for these vessels. Using a double chine rather than single chine reduced the resistance 8%, and reducing the entrance angle reduced the resistance a further 7%. Additional reductions in resistances of 16.6% were achieved with bulbous bows, effective at multiple speeds and in multiple load configurations.

A number of experiments are planned for the UBC series. Seakeeping tests in head seas are currently underway and they will be reported shortly. Standard motion response amplitudes as well as the effect of L/B, B/T and C_b on added resistance and acceleration levels will be studied. Seakeeping tests in oblique waves are planned for later years.

Acknowledgments

The authors would like to thank Energy Mines and Resources and the Department of Fisheries and Oceans of Canada for funding the research program. They also would like to thank Gireesh Sadasivan for his work in designing the parent hull form. Many people assisted in the research project, including especially Bob McIlwaine of Pacific Fisheries R&D Ltd., Gerry Rohling, and George Roddan of BC Research Ocean Engineering Centre.

References

1 Calisal, S.M., McGreer, D., and Rohling, G.F., "A Fishing Vessel Energy Analysis Program," MARINE TECHNOLOGY, Vol. 26, No. 1, Jan. 1989, pp. 62–73.

2 Pattullo, R.N.M. and Thomson, G.R., "The BSRA Trawler Series (Part I)," *Transactions,* RINA, Vol. 107, 1965, pp. 215–241.

3 Pattullo, R.N.M., "The BSRA Trawler Series (Part II)," *Transactions,* RINA, Vol. 110, 1968, pp. 151–185.

4 Ridgley-Nevitt, C., "The Resistance of Trawler Hull Forms of .65 Prismatic Coefficient," *Transactions,* SNAME, Vol. 64, 1956, pp. 433–468.

5 Ridgley-Nevitt, C., "The Development of Parent Hulls for a High Displacement-Length Series of Trawler Forms," *Transactions,* SNAME, Vol. 71, 1963, pp. 5–30.

6 Ridgley-Nevitt, C., "The Resistance of a High Displacement-Length Ratio Trawler Series," *Transactions,* SNAME, Vol. 75, 1967, pp. 51–77.

7 Kafali, K., "A Study on the Fishing Vessel Forms," Turkish Ship Research Institute, Publication No. 25, Technical Univ. of Istanbul, 1980.

8 Van Oortmerssen, G., "A Power Prediction Method and Its Application to Small Ships," *International Shipbuilding Progress,* 1971.

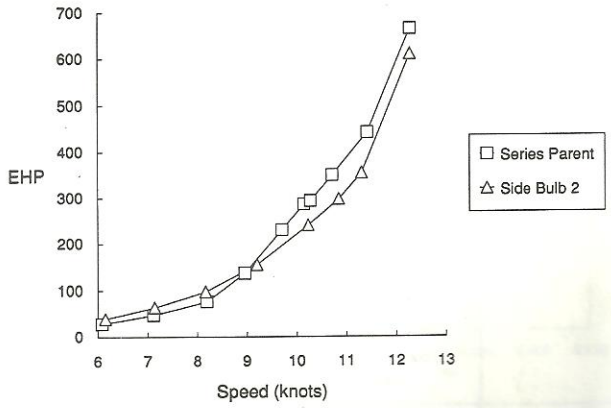

Fig. 10 Resistance of UBC Series parent with side bulb 2

9 Goren, O. and Calisal, S.M., "Optimal Hull Forms for Fishing Vessels," *Thirteenth STAR Symposium,* SNAME, 1988, pp. 41–51.
10 *Principles of Naval Architecture,* 2nd rev., E.V. Lewis, Ed., Vol. 2, SNAME, 1988.
11 Molinaeux, D., Private communications.
12 Weinblum, G.P., "Schiffe Geringsten Widerstandes," *Jahrbuch Shiffbautechnik Gesellschaft,* Vol. 51, 1957, pp. 175–204.
13 Susuki, K., Calisal, S.M., and Tamashima, M., "Hull Form Improvements of Fishing Vessels by Non-Protruding Bow Bulb," Society of Naval Architects of Japan, 1991.
14 Calisal, S.M., Goren, O, and McGreer, D., "Economie de Carburant pour Navires de Peches," Association Technique Maritime et Aeronautique 90th Session, April 1990.
15 Hsiung, C.C., "Optimal Ship Forms for Minimum Wave Resistance," *Journal of Ship Research,* Vol. 28, No. 2, June 1981, pp. 96–116.

Appendix 1 Offsets and sectional area curve for UBC Series parent hull

Table of Offsets
Offsets are nondimensionalized by B/2

Item	Height	Sta 10	Sta 9 1/2	Sta 9	Sta 8 1/2	Sta 8	Sta 7	Sta 6	Sta 5	Sta 4	Sta 3	Sta 2	Sta 1	Sta 0
WL 2	0.078	0.000	0.000	0.000	0.000	0.009	0.189	0.346	0.482	0.424	0.103	0.000	0.000	0.000
WL 3	0.186	0.000	0.081	0.196	0.287	0.375	0.553	0.780	0.859	0.837	0.533	0.000	0.000	0.000
WL 4	0.296	0.000	0.133	0.258	0.385	0.500	0.709	0.868	0.946	0.933	0.846	0.414	0.000	0.000
WL 5	0.404	0.000	0.152	0.287	0.423	0.552	0.763	0.912	0.956	0.957	0.944	0.814	0.052	0.000
WL 6	0.513	0.000	0.159	0.305	0.447	0.577	0.800	0.922	0.963	0.964	0.953	0.929	0.586	0.000
WL 7	0.622	0.000	0.161	0.319	0.460	0.595	0.812	0.932	0.972	0.972	0.962	0.944	0.872	0.011
DWL	1.000	0.000	0.187	0.359	0.513	0.649	0.852	0.967	1.000	0.999	0.994	0.984	0.968	0.938
Lower Chine		0.000	0.163	0.320	0.455	0.569	0.722	0.793	0.815	0.817	0.810	0.799	0.786	0.770
Upper Chine		0.000	0.165	0.322	0.468	0.600	0.797	0.908	0.946	0.949	0.943	0.933	0.923	0.909
Main Deck		0.150	0.298	0.441	0.574	0.694	0.874	0.979	1.008	1.007	1.007	1.007	1.007	1.007

Table of Heights
Heights are nondimensionalized by T

Item	Sta 10	Sta 9 1/2	Sta 9	Sta 8 1/2	Sta 8	Sta 7	Sta 6	Sta 5	Sta 4	Sta 3	Sta 2	Sta 1	Sta 0
Profile	0.324	0.120	0.104	0.087	0.077	0.050	0.021	0.000	-0.013	0.053	0.195	0.393	0.619
Lower Chine	0.802	0.722	0.634	0.552	0.469	0.310	0.192	0.135	0.164	0.255	0.389	0.552	0.757
Upper Chine	0.993	0.906	0.834	0.736	0.650	0.484	0.352	0.293	0.314	0.402	0.518	0.662	0.843
Main Deck	1.539	1.479	1.419	1.361	1.308	1.216	1.148	1.117	1.114	1.144	1.216	1.292	1.380

Sectional Area Curve
Areas are nondimensionalized by Midship Area

Sta 10	Sta 9 1/2	Sta 9	Sta 8 1/2	Sta 8	Sta 7	Sta 6	Sta 5	Sta 4	Sta 3	Sta 2	Sta 1	Sta 0
0.000	0.147	0.293	0.430	0.558	0.775	0.931	1.000	0.992	0.902	0.751	0.538	0.307

Appendix 2 Results of resistance algorithms versus model test results for UBC Series

Model 1 at Loaded Draft Temp = 15.0 C

Fn	Ct	Cf	Cr	Cr (eqn 1)	Cr (eqn 2)
0.216	0.0086	0.0046	0.0041	0.0032	0.0027
0.250	0.0086	0.0044	0.0042	0.0041	0.0038
0.286	0.0090	0.0043	0.0047	0.0055	0.0050
0.288	0.0089	0.0043	0.0046	0.0056	0.0051
0.322	0.0124	0.0042	0.0083	0.0073	0.0066
0.323	0.0127	0.0042	0.0086	0.0073	0.0066
0.342	0.0148	0.0041	0.0107	0.0085	0.0076
0.360	0.0147	0.0041	0.0106	0.0098	0.0088
0.361	0.0150	0.0041	0.0109	0.0098	0.0088
0.362	0.0153	0.0041	0.0112	0.0099	0.0089
0.378	0.0149	0.0041	0.0109	0.0111	0.0101
0.378	0.0152	0.0041	0.0111	0.0111	0.0101
0.394	0.0166	0.0040	0.0126	0.0123	0.0114
0.394	0.0169	0.0040	0.0129	0.0123	0.0114
0.431	0.0201	0.0039	0.0161	0.0153	0.0156

Fig. 11

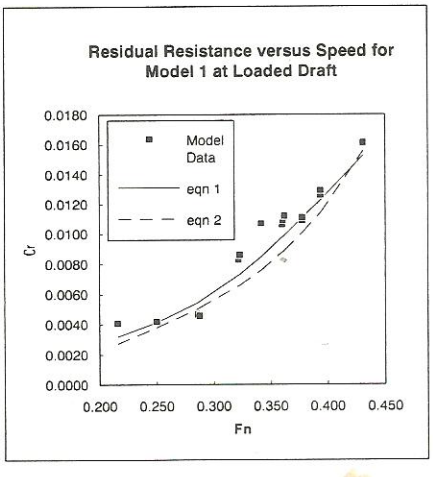

Model 2 at Loaded Draft Temp = 17.6 C

Fn	Ct	Cf	Cr	Cr (eqn 1)	Cr (eqn 2)
0.191	0.0091	0.0049	0.0043	0.0029	0.0032
0.210	0.0096	0.0048	0.0049	0.0035	0.0036
0.229	0.0094	0.0047	0.0047	0.0040	0.0041
0.249	0.0095	0.0046	0.0049	0.0046	0.0046
0.269	0.0095	0.0045	0.0050	0.0053	0.0053
0.294	0.0112	0.0044	0.0067	0.0064	0.0063
0.309	0.0118	0.0044	0.0074	0.0072	0.0070
0.328	0.0141	0.0043	0.0097	0.0083	0.0080
0.351	0.0157	0.0043	0.0114	0.0098	0.0095
0.370	0.0164	0.0042	0.0122	0.0112	0.0111
0.392	0.0160	0.0042	0.0118	0.0128	0.0131

Fig. 12

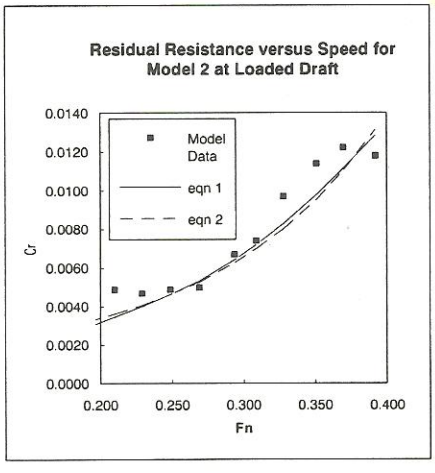

Model 3 at Loaded Draft			Temp = 17.6 C		
Fn	Ct	Cf	Cr	Cr (eqn 1)	Cr (eqn 2)
0.204	0.0065	0.0042	0.0023	0.0017	0.0011
0.220	0.0065	0.0041	0.0024	0.0019	0.0018
0.220	0.0065	0.0041	0.0024	0.0019	0.0018
0.235	0.0070	0.0041	0.0029	0.0022	0.0024
0.251	0.0067	0.0040	0.0027	0.0025	0.0029
0.267	0.0075	0.0040	0.0036	0.0030	0.0034
0.283	0.0075	0.0039	0.0036	0.0035	0.0039
0.297	0.0082	0.0039	0.0043	0.0041	0.0043
0.317	0.0095	0.0038	0.0056	0.0051	0.0050
0.331	0.0121	0.0038	0.0083	0.0059	0.0056
0.345	0.0124	0.0038	0.0086	0.0068	0.0062
0.360	0.0136	0.0037	0.0099	0.0077	0.0069
0.376	0.0136	0.0037	0.0099	0.0089	0.0079
0.393	0.0141	0.0037	0.0104	0.0103	0.0091
0.407	0.0149	0.0036	0.0112	0.0114	0.0103

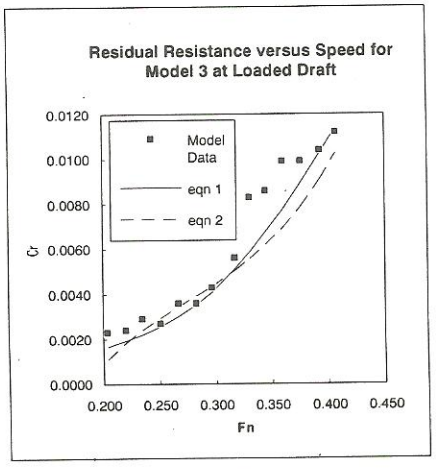

Fig. 13

Model 4 at Loaded Draft			Temp = 18.5 C		
Fn	Ct	Cf	Cr	Cr (eqn 1)	Cr (eqn 2)
0.216	0.0085	0.0045	0.0040	0.0038	0.0025
0.252	0.0080	0.0043	0.0037	0.0049	0.0038
0.294	0.0099	0.0042	0.0057	0.0066	0.0053
0.324	0.0128	0.0041	0.0086	0.0083	0.0066
0.343	0.0146	0.0041	0.0105	0.0095	0.0077
0.358	0.0158	0.0040	0.0118	0.0106	0.0086
0.358	0.0159	0.0040	0.0118	0.0106	0.0086
0.380	0.0166	0.0040	0.0126	0.0123	0.0103
0.398	0.0178	0.0039	0.0139	0.0137	0.0118
0.432	0.0212	0.0039	0.0174	0.0165	0.0159

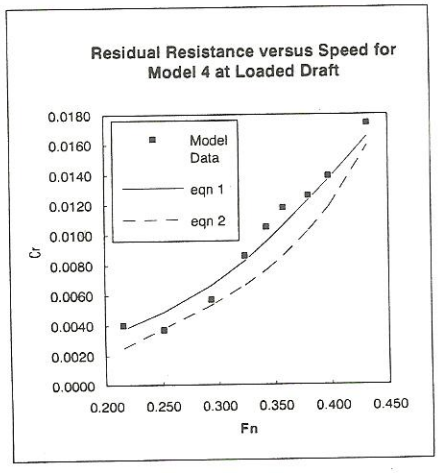

Fig. 14

Model 5 at Loaded Draft			Temp = 17.2 C		
Fn	Ct	Cf	Cr	Cr (eqn 1)	Cr (eqn 2)
0.214	0.0117	0.0045	0.0072	0.0049	0.0065
0.250	0.0110	0.0044	0.0066	0.0062	0.0063
0.283	0.0120	0.0042	0.0077	0.0077	0.0075
0.303	0.0132	0.0042	0.0090	0.0088	0.0083
0.322	0.0164	0.0041	0.0123	0.0099	0.0093
0.339	0.0177	0.0041	0.0136	0.0110	0.0104
0.356	0.0193	0.0041	0.0153	0.0123	0.0116
0.377	0.0192	0.0040	0.0152	0.0138	0.0134
0.397	0.0188	0.0040	0.0148	0.0155	0.0155
0.409	0.0208	0.0039	0.0168	0.0165	0.0170
0.428	0.0236	0.0039	0.0197	0.0181	0.0196

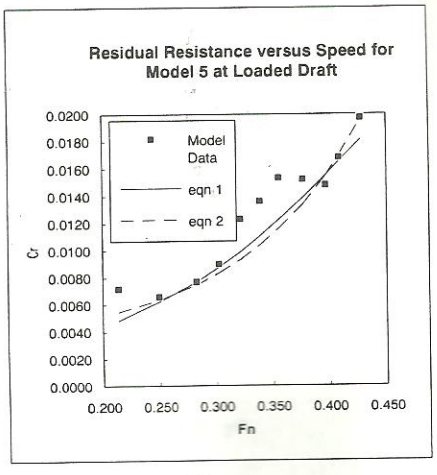

Fig. 15

Model 6 at Loaded Draft			Temp = 16.1 C		
Fn	Ct	Cf	Cr	Cr (eqn 1)	Cr (eqn 2)
0.193	0.0073	0.0043	0.0030	0.0020	0.0018
0.219	0.0074	0.0042	0.0032	0.0025	0.0031
0.249	0.0076	0.0040	0.0036	0.0032	0.0041
0.281	0.0080	0.0039	0.0041	0.0043	0.0050
0.300	0.0091	0.0039	0.0052	0.0051	0.0055
0.310	0.0102	0.0039	0.0063	0.0056	0.0058
0.314	0.0109	0.0039	0.0070	0.0058	0.0059
0.328	0.0124	0.0038	0.0086	0.0066	0.0064
0.344	0.0134	0.0038	0.0096	0.0076	0.0070
0.364	0.0140	0.0038	0.0103	0.0090	0.0080
0.378	0.0145	0.0037	0.0108	0.0101	0.0088
0.393	0.0151	0.0037	0.0114	0.0113	0.0099
0.408	0.0161	0.0037	0.0124	0.0125	0.0112
0.440	0.0195	0.0036	0.0159	0.0153	0.0150

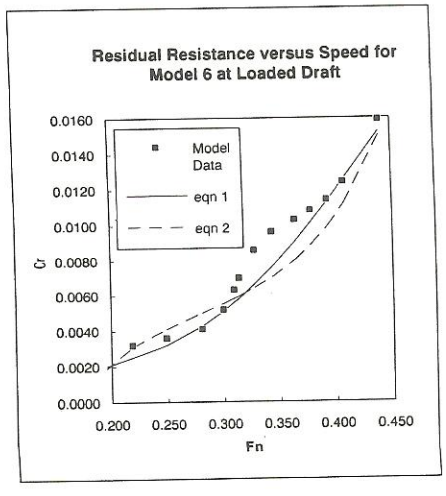

Fig. 16

Model 7 at Loaded Draft			Temp = 16.1 C		
Fn	Ct	Cf	Cr	Cr (eqn 1)	Cr (eqn 2)
0.210	0.0070	0.0045	0.0025	0.0013	0.0028
0.247	0.0074	0.0044	0.0030	0.0019	0.0041
0.284	0.0076	0.0043	0.0033	0.0027	0.0055
0.302	0.0079	0.0042	0.0037	0.0034	0.0063
0.322	0.0091	0.0042	0.0049	0.0043	0.0073
0.337	0.0095	0.0041	0.0054	0.0051	0.0081
0.356	0.0102	0.0041	0.0061	0.0063	0.0094
0.356	0.0101	0.0041	0.0060	0.0063	0.0094
0.376	0.0113	0.0040	0.0073	0.0077	0.0110
0.396	0.0139	0.0040	0.0099	0.0093	0.0129
0.410	0.0160	0.0040	0.0120	0.0104	0.0145
0.427	0.0198	0.0039	0.0159	0.0119	0.0168
0.468	0.0309	0.0039	0.0271	0.0155	0.0241

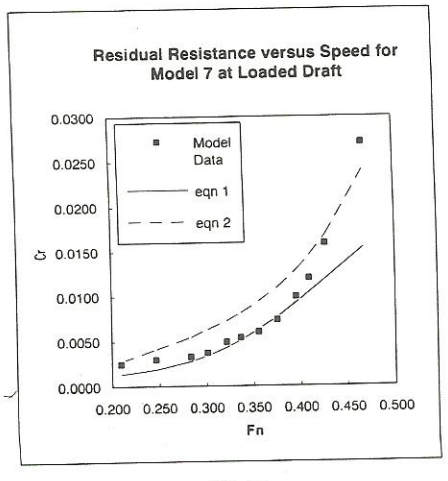

Fig. 17

Model 8 at Loaded Draft			Temp = 16.1 C		
Fn	Ct	Cf	Cr	Cr (eqn 1)	Cr (eqn 2)
0.189	0.0055	0.0043	0.0012	0.0011	0.0003
0.221	0.0049	0.0041	0.0007	0.0015	0.0021
0.256	0.0058	0.0040	0.0018	0.0020	0.0034
0.285	0.0062	0.0039	0.0022	0.0025	0.0044
0.319	0.0070	0.0039	0.0031	0.0036	0.0056
0.348	0.0082	0.0038	0.0045	0.0048	0.0070
0.380	0.0096	0.0037	0.0059	0.0065	0.0090
0.413	0.0126	0.0037	0.0089	0.0094	0.0120

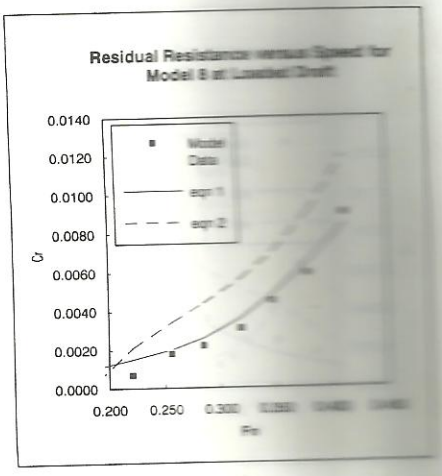

Fig. 18

Model 9 at Loaded Draft			Temp = 16.1 C		
Fn	Ct	Cf	Cr	Cr (eqn 1)	Cr (eqn 2)
0.213	0.0057	0.0045	0.0012	0.0013	0.0024
0.253	0.0059	0.0044	0.0015	0.0019	0.0039
0.286	0.0073	0.0043	0.0031	0.0026	0.0051
0.326	0.0082	0.0042	0.0041	0.0042	0.0069
0.341	0.0094	0.0041	0.0053	0.0050	0.0077
0.363	0.0103	0.0041	0.0062	0.0064	0.0091
0.377	0.0110	0.0040	0.0069	0.0073	0.0101
0.397	0.0126	0.0040	0.0086	0.0088	0.0120
0.409	0.0155	0.0040	0.0115	0.0098	0.0133
0.434	0.0190	0.0039	0.0151	0.0117	0.0165

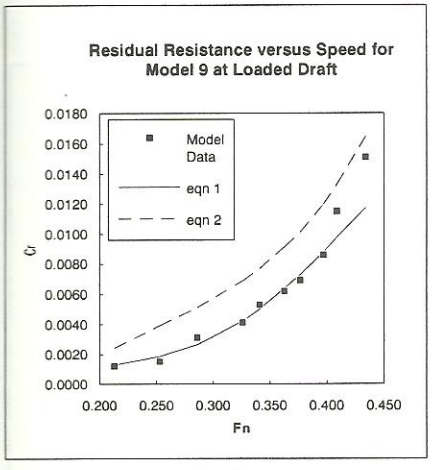

Fig. 19

Model 10 at Loaded Draft			Temp = 16.1 C		
Fn	Ct	Cf	Cr	Cr (eqn 1)	Cr (eqn 2)
0.216	0.0074	0.0045	0.0029	0.0015	0.0054
0.249	0.0072	0.0044	0.0028	0.0021	0.0062
0.290	0.0082	0.0043	0.0039	0.0032	0.0076
0.326	0.0091	0.0042	0.0050	0.0048	0.0093
0.363	0.0109	0.0041	0.0068	0.0072	0.0118
0.401	0.0147	0.0040	0.0107	0.0102	0.0155
0.438	0.0234	0.0039	0.0195	0.0135	0.0208

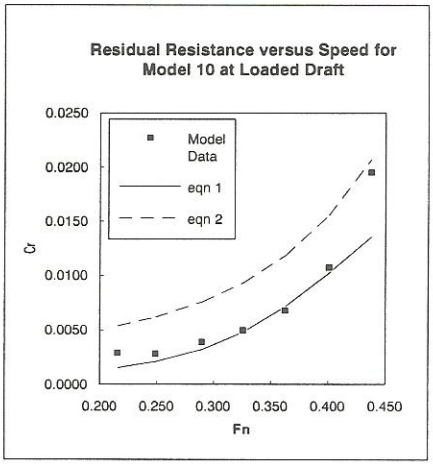

Fig. 20

Model 11 at Loaded Draft			Temp = 16.1 C		
Fn	Ct	Cf	Cr	Cr (eqn 1)	Cr (eqn 2)
0.189	0.0084	0.0043	0.0041	0.0028	0.0005
0.221	0.0073	0.0041	0.0032	0.0037	0.0021
0.254	0.0087	0.0040	0.0047	0.0048	0.0034
0.255	0.0080	0.0040	0.0039	0.0048	0.0034
0.287	0.0088	0.0039	0.0049	0.0061	0.0046
0.318	0.0113	0.0039	0.0075	0.0077	0.0059
0.334	0.0140	0.0038	0.0102	0.0088	0.0068
0.353	0.0157	0.0038	0.0119	0.0100	0.0078
0.386	0.0164	0.0037	0.0127	0.0126	0.0103
0.421	0.0178	0.0037	0.0141	0.0155	0.0140

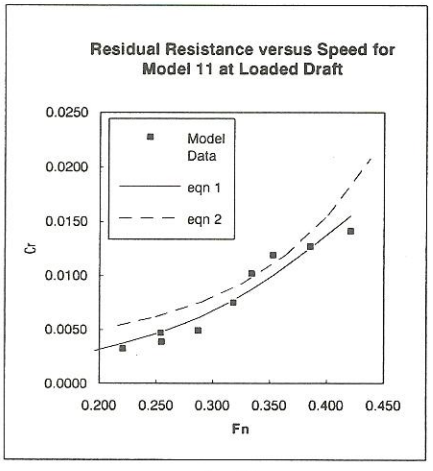

Fig. 21

Model 12 at Loaded Draft			Temp = 16.1 C		
Fn	Ct	Cf	Cr	Cr (eqn 1)	Cr (eqn 2)
0.189	0.0063	0.0043	0.0020	0.0010	0.0016
0.220	0.0061	0.0041	0.0019	0.0014	0.0032
0.255	0.0065	0.0040	0.0025	0.0019	0.0044
0.287	0.0065	0.0039	0.0026	0.0025	0.0053
0.319	0.0075	0.0039	0.0037	0.0034	0.0062
0.353	0.0087	0.0038	0.0049	0.0047	0.0076
0.387	0.0097	0.0037	0.0060	0.0064	0.0096
0.415	0.0123	0.0037	0.0086	0.0079	0.0121

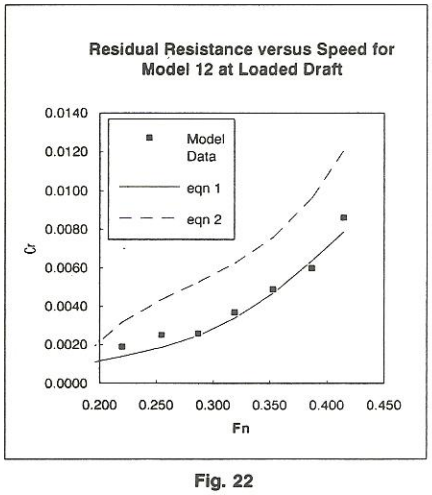

Fig. 22

Model 13 at Loaded Draft			Temp = 16.1 C		
Fn	Ct	Cf	Cr	Cr (eqn 1)	Cr (eqn 2)
0.189	0.0061	0.0043	0.0019	0.0012	0.0005
0.221	0.0063	0.0041	0.0021	0.0016	0.0021
0.254	0.0063	0.0040	0.0023	0.0021	0.0033
0.289	0.0063	0.0039	0.0024	0.0029	0.0046
0.318	0.0077	0.0039	0.0039	0.0039	0.0058
0.349	0.0096	0.0038	0.0058	0.0053	0.0074
0.384	0.0107	0.0037	0.0070	0.0072	0.0099
0.412	0.0136	0.0037	0.0099	0.0089	0.0126

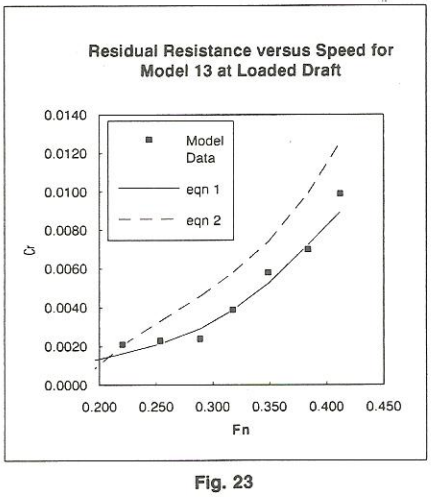

Fig. 23

Model 1 at Lightship Draft			Temp = 21.0 C	
Fn	Ct	Cf	Cr	Cr (eqn 3)
0.218	0.0061	0.0044	0.0017	0.0013
0.252	0.0064	0.0043	0.0021	0.0017
0.290	0.0068	0.0041	0.0027	0.0025
0.326	0.0083	0.0041	0.0043	0.0036
0.372	0.0103	0.0039	0.0063	0.0060
0.403	0.0127	0.0039	0.0089	0.0085
0.419	0.0154	0.0039	0.0115	0.0102
0.464	0.0242	0.0038	0.0204	0.0173

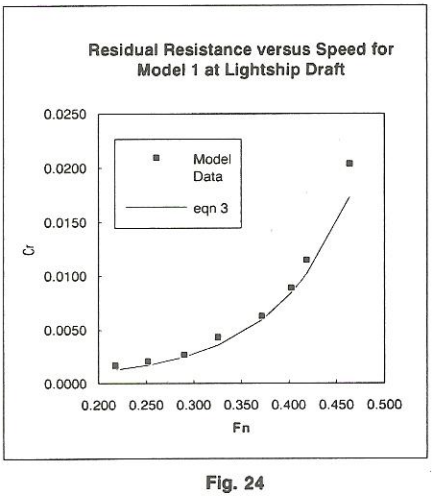

Fig. 24

Model 2 at Lightship Draft	Temp = 17.2 C			
Fn	Ct	Cf	Cr	Cr (eqn 3)
0.232	0.0069	0.0047	0.0022	0.0016
0.276	0.0077	0.0045	0.0032	0.0024
0.282	0.0075	0.0045	0.0030	0.0026
0.284	0.0075	0.0045	0.0030	0.0026
0.314	0.0086	0.0044	0.0042	0.0036
0.352	0.0101	0.0043	0.0058	0.0055
0.353	0.0099	0.0043	0.0056	0.0056
0.374	0.0109	0.0042	0.0067	0.0070
0.395	0.0130	0.0042	0.0088	0.0088
0.410	0.0153	0.0041	0.0111	0.0104
0.415	0.0160	0.0041	0.0119	0.0109
0.431	0.0196	0.0041	0.0155	0.0130
0.452	0.0240	0.0041	0.0200	0.0163
0.476	0.0310	0.0040	0.0270	0.0212

Model 3 at Lightship Draft	Temp = 17.2 C			
Fn	Ct	Cf	Cr	Cr (eqn 3)
0.219	0.0053	0.0041	0.0012	0.0011
0.257	0.0059	0.0040	0.0019	0.0014
0.282	0.0061	0.0039	0.0022	0.0018
0.299	0.0066	0.0039	0.0027	0.0021
0.298	0.0056	0.0039	0.0017	0.0020
0.335	0.0082	0.0038	0.0044	0.0030
0.350	0.0081	0.0038	0.0044	0.0035
0.368	0.0089	0.0037	0.0052	0.0044
0.379	0.0094	0.0037	0.0057	0.0050
0.400	0.0112	0.0037	0.0076	0.0066
0.411	0.0124	0.0036	0.0088	0.0077
0.426	0.0137	0.0036	0.0100	0.0094
0.435	0.0153	0.0036	0.0117	0.0107
0.454	0.0175	0.0036	0.0139	0.0138
0.480	0.0200	0.0035	0.0165	0.0197

Model 4 at Lightship Draft	Temp = 17.1 C			
Fn	Ct	Cf	Cr	Cr (eqn 3)
0.216	0.0056	0.0045	0.0011	0.0013
0.250	0.0066	0.0044	0.0023	0.0017
0.287	0.0067	0.0042	0.0025	0.0023
0.324	0.0073	0.0041	0.0032	0.0032
0.362	0.0093	0.0040	0.0053	0.0049
0.398	0.0117	0.0040	0.0077	0.0074
0.436	0.0173	0.0039	0.0134	0.0115
0.470	0.0229	0.0038	0.0191	0.0176
0.506	0.0302	0.0038	0.0264	0.0275
0.546	0.0458	0.0037	0.0421	0.0451

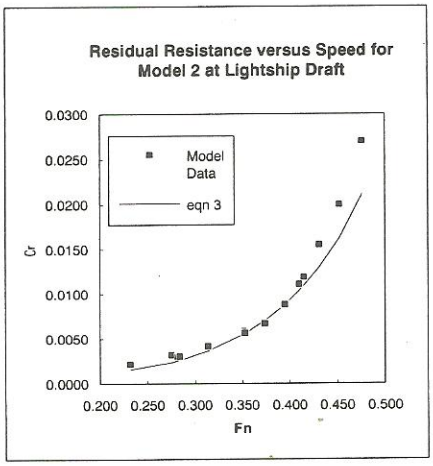

Fig. 25

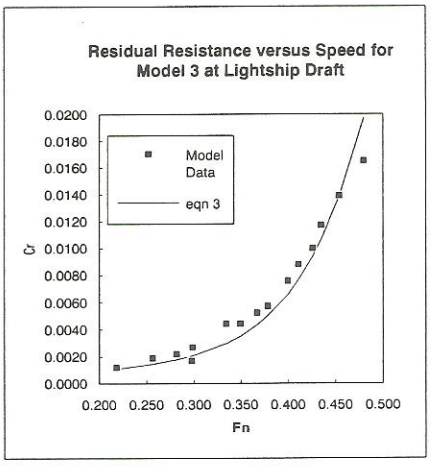

Fig. 26

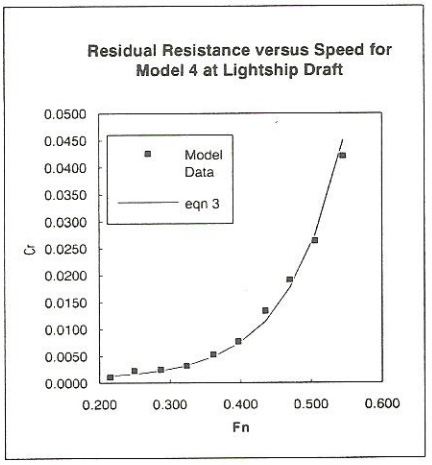

Fig. 27

Model 5 at Lightship Draft	Temp = 17.3 C			
Fn	Ct	Cf	Cr	Cr (eqn 3)
0.218	0.0058	0.0045	0.0013	0.0015
0.247	0.0065	0.0044	0.0021	0.0019
0.274	0.0068	0.0043	0.0025	0.0024
0.322	0.0088	0.0041	0.0047	0.0040
0.366	0.0102	0.0040	0.0062	0.0063
0.400	0.0133	0.0040	0.0093	0.0091
0.435	0.0204	0.0039	0.0165	0.0135
0.472	0.0287	0.0038	0.0249	0.0202
0.507	0.0385	0.0038	0.0347	0.0300
0.547	0.0469	0.0037	0.0432	0.0471

Model 6 at Lightship Draft	Temp = 17.1 C			
Fn	Ct	Cf	Cr	Cr (eqn 3)
0.223	0.0053	0.0041	0.0011	0.0014
0.253	0.0058	0.0040	0.0018	0.0016
0.285	0.0060	0.0039	0.0021	0.0019
0.318	0.0071	0.0038	0.0032	0.0024
0.351	0.0083	0.0038	0.0045	0.0034
0.380	0.0088	0.0037	0.0051	0.0047
0.416	0.0120	0.0036	0.0084	0.0078
0.446	0.0147	0.0036	0.0111	0.0118
0.476	0.0164	0.0035	0.0129	0.0183

Model 7 at Lightship Draft	Temp = 19.8 C			
Fn	Ct	Cf	Cr	Cr (eqn 3)
0.212	0.0058	0.0045	0.0013	0.0014
0.235	0.0056	0.0044	0.0012	0.0016
0.282	0.0067	0.0042	0.0025	0.0025
0.312	0.0070	0.0041	0.0029	0.0035
0.350	0.0075	0.0040	0.0035	0.0052
0.369	0.0090	0.0040	0.0050	0.0064
0.392	0.0118	0.0039	0.0079	0.0083
0.427	0.0173	0.0039	0.0134	0.0125
0.467	0.0259	0.0038	0.0221	0.0199
0.479	0.0287	0.0038	0.0250	0.0230
0.503	0.0331	0.0037	0.0294	0.0306
0.542	0.0394	0.0037	0.0357	0.0483

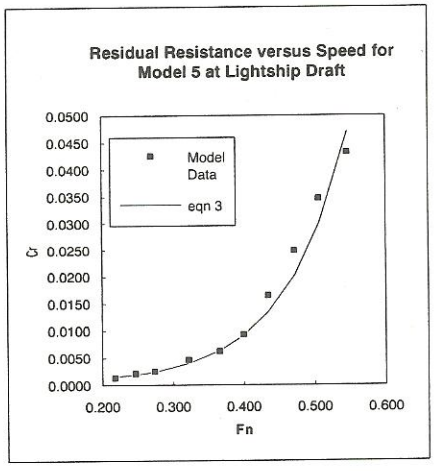

Fig. 28

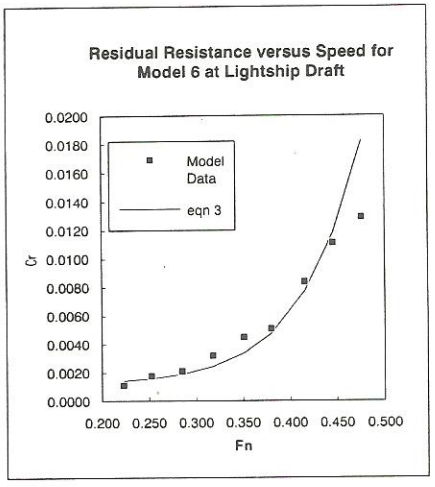

Fig. 29

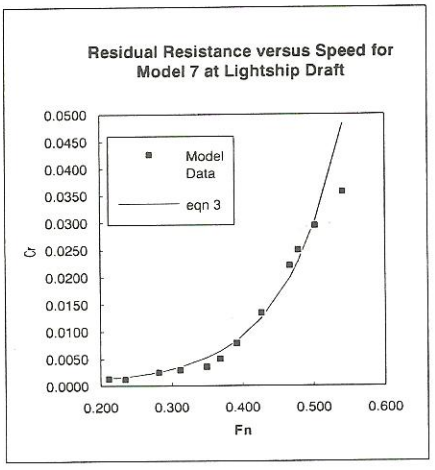

Fig. 30

Model 8 at Lightship Draft			Temp = 17.3 C	
Fn	Ct	Cf	Cr	Cr (eqn 3)
0.224	0.0051	0.0041	0.0010	0.0013
0.254	0.0056	0.0040	0.0016	0.0016
0.289	0.0056	0.0039	0.0017	0.0021
0.316	0.0060	0.0038	0.0022	0.0027
0.351	0.0063	0.0038	0.0025	0.0040
0.383	0.0080	0.0037	0.0043	0.0059
0.414	0.0108	0.0036	0.0071	0.0088
0.445	0.0148	0.0036	0.0112	0.0135
0.478	0.0203	0.0035	0.0168	0.0213

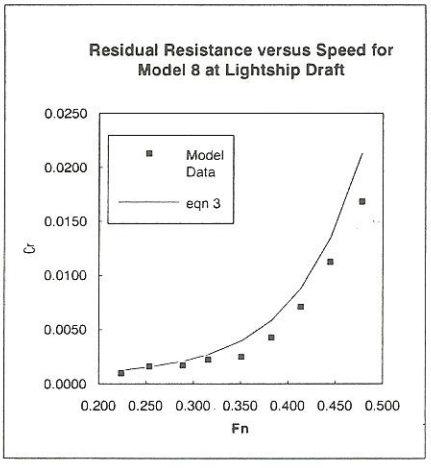

Fig. 31

Model 9 at Lightship Draft			Temp = 20.0 C	
Fn	Ct	Cf	Cr	Cr (eqn 3)
0.214	0.0060	0.0044	0.0015	0.0015
0.254	0.0063	0.0043	0.0020	0.0019
0.293	0.0066	0.0042	0.0025	0.0027
0.332	0.0069	0.0041	0.0028	0.0039
0.359	0.0079	0.0040	0.0039	0.0052
0.400	0.0112	0.0039	0.0073	0.0083
0.435	0.0167	0.0038	0.0129	0.0127
0.443	0.0173	0.0038	0.0135	0.0140
0.454	0.0196	0.0038	0.0158	0.0159
0.497	0.0264	0.0037	0.0227	0.0275
0.503	0.0268	0.0037	0.0231	0.0295
0.540	0.0396	0.0037	0.0359	0.0468

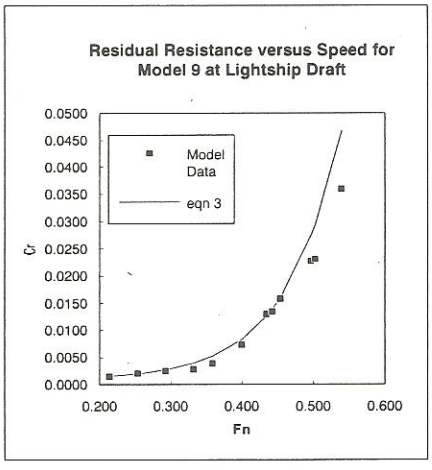

Fig. 32

Model 10 at Lightship Draft			Temp = 17.3 C	
Fn	Ct	Cf	Cr	Cr (eqn 3)
0.215	0.0060	0.0045	0.0015	0.0017
0.252	0.0065	0.0043	0.0022	0.0021
0.289	0.0066	0.0042	0.0024	0.0031
0.329	0.0076	0.0041	0.0035	0.0047
0.371	0.0093	0.0040	0.0053	0.0074
0.402	0.0138	0.0040	0.0098	0.0103
0.440	0.0214	0.0039	0.0175	0.0156
0.468	0.0280	0.0038	0.0242	0.0212
0.508	0.0372	0.0038	0.0334	0.0332
0.549	0.0434	0.0037	0.0397	0.0525

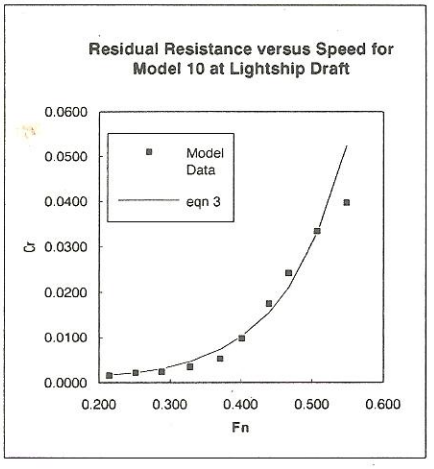

Fig. 33

Model 11 at Lightship Draft			Temp = 17.3 C	
Fn	Ct	Cf	Cr	Cr (eqn 3)
0.221	0.0053	0.0041	0.0012	0.0010
0.252	0.0057	0.0040	0.0017	0.0013
0.284	0.0061	0.0039	0.0022	0.0019
0.317	0.0077	0.0038	0.0038	0.0027
0.350	0.0087	0.0038	0.0050	0.0039
0.378	0.0099	0.0037	0.0062	0.0055
0.413	0.0127	0.0036	0.0091	0.0085
0.446	0.0180	0.0036	0.0144	0.0130
0.480	0.0236	0.0035	0.0200	0.0202

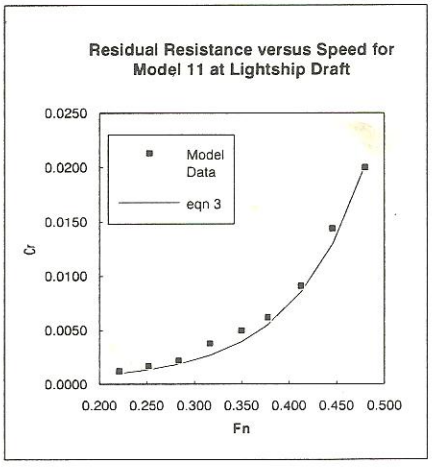

Fig. 34

Model 12 at Lightship Draft			Temp = 17.3 C	
Fn	Ct	Cf	Cr	Cr (eqn 3)
0.214	0.0052	0.0041	0.0011	0.0015
0.255	0.0053	0.0040	0.0013	0.0018
0.280	0.0056	0.0039	0.0017	0.0021
0.311	0.0058	0.0038	0.0020	0.0026
0.354	0.0068	0.0038	0.0030	0.0039
0.375	0.0077	0.0037	0.0040	0.0050
0.412	0.0108	0.0036	0.0072	0.0082
0.440	0.0135	0.0036	0.0099	0.0122
0.469	0.0199	0.0036	0.0164	0.0185
0.475	0.0182	0.0035	0.0146	0.0201

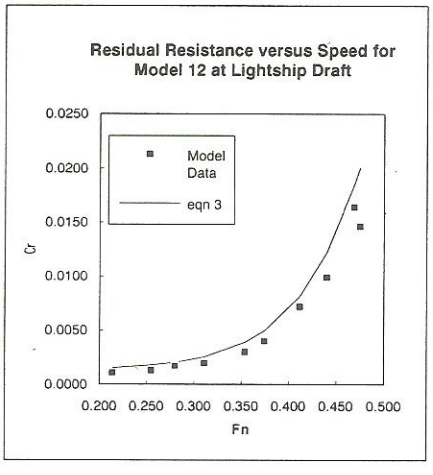

Fig. 35

Model 13 at Lightship Draft			Temp = 17.3 C	
Fn	Ct	Cf	Cr	Cr (eqn 1)
0.222	0.0053	0.0041	0.0012	0.0011
0.252	0.0054	0.0040	0.0014	0.0015
0.284	0.0054	0.0039	0.0015	0.0021
0.317	0.0061	0.0038	0.0023	0.0029
0.351	0.0068	0.0038	0.0030	0.0044
0.376	0.0080	0.0037	0.0042	0.0059
0.409	0.0112	0.0036	0.0075	0.0090
0.443	0.0166	0.0036	0.0130	0.0137
0.475	0.0211	0.0035	0.0175	0.0208

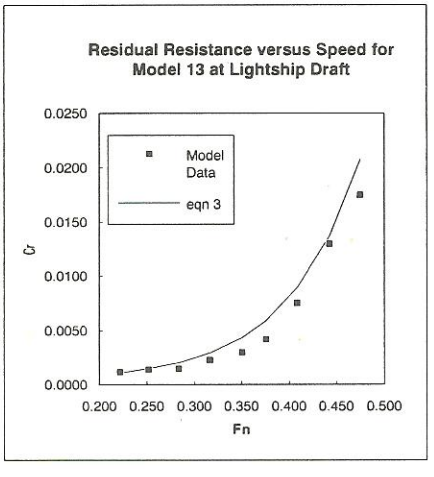

Fig. 36